

## ***T* waves from the great 1994 Bolivian deep earthquake in relation to channeling of *S* wave energy up the slab**

Emile A. Okal

Department of Geological Sciences, Northwestern University, Evanston, Illinois

Jacques Talandier

Laboratoire de Détection et Géophysique, Commissariat à l'Énergie Atomique, Bruyères-le-Châtel, France

**Abstract.** We report the observation of *T* phases recorded at a number of Pacific island sites, following the great Bolivian deep earthquake of June 9, 1994. By studying their arrival times at the various stations, we unravel the process of conversion from seismic to acoustic energy at the South American coastline. We find that the maxima of amplitude of the phase are incompatible with propagation along the great circle from source to receiver but rather require the generation of the acoustic wave at a common point at the Arica Bight for all stations in the South Pacific, and even farther south for stations in Hawaii and the Bonin Islands. The timing of these conversions corresponds to the arrival of regional *S* waves at the conversion points. The high-frequency nature of the *T* phase requires the channeling of the *S* wave from the seismic source to conversion point through low-attenuation material, which in turn adds supportive evidence for the mechanical continuity of the downgoing slab under that section of South America, despite the observed gap in seismicity between 300 and 600 km.

### **Introduction**

*T* waves, propagating over large distances in the low-velocity SOFAR channel of the ocean column [Jensen *et al.*, 1994, p. 23], can be generated not only by marine sources but also by earthquakes, when seismic waves excited in the solid Earth hit the ocean boundary, and a fraction of their energy is transformed to acoustic energy in the water. We refer to Talandier and Okal [1997] for a detailed study of this process, and of the conversion back to seismic energy when the *T* wave reaches an island shore. The latter, also investigated by Koyanagi *et al.* [1995] and McLaughlin [1997], allows the routine recording of *T* phases by seismometers located on islands and, in particularly favorable cases, the actual feeling of *T* phases by island populations [Talandier and Okal, 1979].

Since the *T* wave is guided through the narrow SOFAR channel, its spectrum is restricted to high frequencies, in practice,  $f \geq 2$  Hz. Due to the generally strong attenuation of *P* or *S* waves at such frequencies, one would expect earthquake *T* phases to be generated preferentially by seismic sources in the immediate vicinity of coastlines and, in particular, only by shallow events. However, under favorable conditions, intermediate-depth or even deep sources have generated substantial *T* waves, and indeed one of the first correct descriptions of teleseismic records of *T* waves possibly involved earthquakes of intermediate depth [Linehan, 1940]. Following the great 1970 Colombian earthquake, *T* waves were recorded in Polynesia; we briefly analyze one such record in this study.

We focus here on *T* phases recorded at Pacific island sites following the great Bolivian deep earthquake of June 9, 1994. We will show that the timing of the amplitude maxima of these wave trains require that they were generated at the Arica Bight (the "elbow" in the South American coastline at the Peru-Chile border) or farther South in the case of northern Pacific island stations, in both instances at a time consistent with the arrival of *S* waves. The high-frequency nature of this scattering source requires anomalously low attenuation of the corresponding regional *S* waves, thus suggesting their efficient channeling up the slab on a path from the hypocenter to the conversion point, which in turn advocates mechanical continuity of the slab.

### ***T* Phase Dataset and Methods of Study**

Table 1 gives a list of records assembled for the present study. The dataset includes seismograms from both permanent and portable IRIS and POSEIDON digital stations, from the French Polynesia Network (RSP), and from the HVO network on the Big Island of Hawaii. Some RSP records are also available in digital form. Our goal is to model the timing of the maximum amplitude of the *T* phase at the various stations, in order to unravel their point of origin, both in space and time. The Appendix provides a detailed analysis of each record used in this study and discusses the use of a time correction, if any. In several instances, the record is affected by interesting but complex phenomena, such as masking or multipathing, which prevent the use of a precise arrival time.

The precision with which the arrivals of maximum amplitude can be read is on the order of 5 s. While this uncertainty is large by seismological standards, it is comparable to, if not better than, the typical precision achieved on

Copyright 1997 by the American Geophysical Union.

Paper number 97JB02718.  
0148-0227/97/97JB-02718\$09.00

**Table 1.** *T* Phase Records Used in This Study

Station	Island Group	Code	Network	Distance from Conversion Point (km)	Azimuth from Conversion Point (°)	<i>T</i> Wave Arrival Time (UT)	
						Raw	Corrected
<i>Converted at Arica Bight</i>							
Rapa Nui	Easter	RPN	IRIS	4036	249		no <i>T</i> wave
Rikitea	Gambier	RKT	IRIS	6626	254	0151:04	0151:09
Tubuai	Austral	TBI	RSP	8076	251	0207:24	0207:28
Mehetia	Society	MEH	RSP	8078	256	0207:19	0207:19
Rarotonga	Cook	RAR	IRIS	9162	250	0217:57	converted at Mangaia
Niue	Niue	NIU	SWP	10242	249	0231:36	0231:40
Afiamalau	Samoa	AFI	IRIS	10628	253		obscured by local earthquakes
Nauru	Nauru	NAU	OJP	13355	258	0306:30	0306:30
Kosrae	Caroline	KOS	OJP	13988	263	0313:45	0313:45
<i>Converted at Caleta Buena</i>							
Wahaula	Hawaii	WHA	HVO	10207	290	0231:30	0231:30
Chichi-jima	Bonin	OGS	POS	16619	289	0343:30	0343:30

Network abbreviations are IRIS, Incorporated Research Institutions in Seismology; RSP, Réseau Sismique Polynésien; SWP, Southwest Pacific PASSCAL experiment [Wiens *et al.*, 1994]; OJP, Ontong-Java PASSCAL experiment [Richardson and Okal, 1996]; HVO, Hawaiian Volcano Observatory Network; POS, POSEIDON Network.

teleseismic *P* wave arrivals, when scaled by the appropriate slowness (0.67 s/km for *T* waves; typically 0.07 s/km for *P* waves).

We did not attempt to study the amplitude of the *T* phases recorded at island stations, since the latter is controlled in large part by the conversion process and the subsequent inland propagation.

#### General Characteristics of the *T* Phase

*T* phases from the Bolivian earthquake were recorded as far as Chichi-jima, Bonin Islands, more than 16,600 km from the coast of South America. In itself, this is not surprising since SOFAR propagation is known for its exceptional efficiency. In addition, the relevant great circle paths avoid most island groups which could reflect the waves.

The most spectacular examples of *T* phases from the Bolivian earthquake are obtained on paper records from short-period HVO and RSP stations. The advantage of using such instruments in the study of *T* waves comes from the elimination of the ambient noise at frequencies on the order of 0.15 to 0.3 Hz, which finds its origin in sea swell, and is known to plague time-domain broadband records at island stations. In this respect, the RSP features a so-called "*T*-wave channel" which uses a combination of high-pass and band rejection filters, allowing magnifications as high as  $2 \times 10^6$  at 3 Hz [Talandier and Kuster, 1976].

Figure 1 shows the short-period record at Heiheiiahulu (HUL), 7 km from the southeastern coast of the Big Island of Hawaii. The *T* phase is also well recorded at other HVO stations farther inland, such as DES (11 km from the coast), and even emerges from the background noise at MLO, on the flanks of Mauna Loa, 35 km from the shore.

The *T* wave at HUL starts around 0226 UT as a very emergent signal which builds up slowly and reaches a sustained maximum lasting from about 0230 to 0232:10. It then quickly subsides and becomes very small by 0234:15. While this record has a remarkable signal-to-noise ratio, it is

relatively difficult to pick an arrival time for maximum amplitude, possibly due to the location of the station 7 km inland, which probably results in multipathing through several acoustic-to-seismic conversion points. For this reason, we prefer using the seismogram at Wahaula (WHA), a few hundred meters from the coast line where, despite higher background noise, the record has similar characteristics, but with a clearer maximum of amplitude at 0231:30 UT.

#### Spectrograms

For those data available in digital form, a particularly effective tool consists of computing spectrograms, representing contours of the spectral amplitude of the wave as a function of frequency in a time domain window moving across the available seismogram. Figure 2 shows a spectrogram of the record at RSP station MEH, together with a plot of the original seismogram. The most intense arrival for  $3.25 \leq f \leq 5.5$  Hz occurs at 0207:15 UT, or 255 s into the record. While this agrees with the shape of the record in the time domain, this method is clearly superior for the selection of a precise arrival time.

In turn, spectrograms can be used for those stations where the *T* arrival is drowned into lower-frequency background noise, such as the more distant broadband IRIS stations RAR, AFI, KOS, NAU. Systematic filtering of digital records using interactive software is also a powerful tool to extract and identify *T* phases.

#### Acoustic-to-Seismic Conversions and Station Corrections

The recording of *T* phases at various Pacific islands illustrates the efficient acoustic-to-seismic conversions at their shores. As discussed more in detail by Talandier and Okal [1997], high islands or atolls featuring a steep coral reef (with slopes approaching 50°) are particularly efficient con-

## Heiheiahulu (HUL) — 09 June 1994

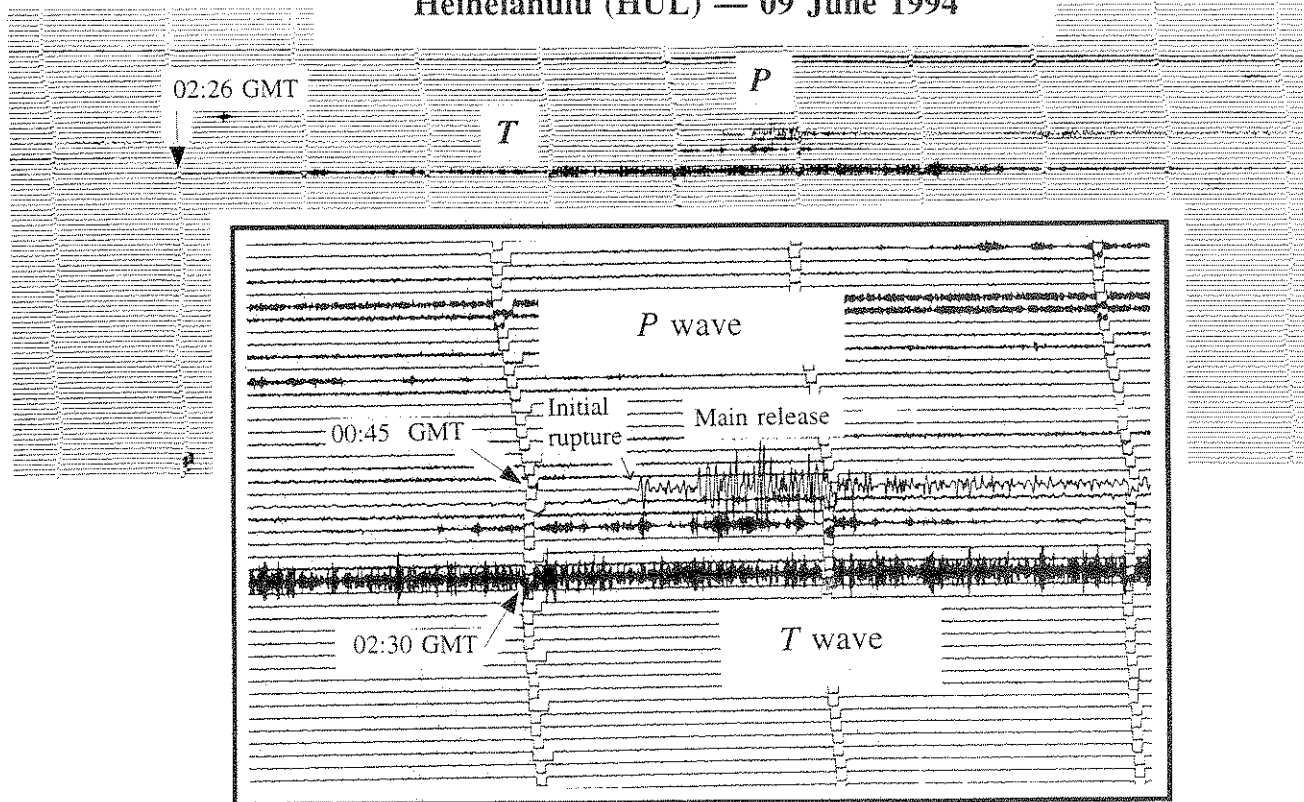


**Figure 1.** Original short-period record at Heiheiahulu, Hawaii, showing the prominent *T* phase from the great Bolivian earthquake. The inset shows a close-up of the central part of the record. Note that the main moment release occurs about 25 s into the source. Ticks are minute marks; there are four lines to the hour. The signal around 0130 UT is probably volcanic tremor, unassociated with the Bolivian event.

verters. This is certainly the case for Polynesian and Cook Island stations TBI and NIU, and for the more distant Micronesian stations, NAU and KOS. In the above geometries, the small scale of the island also minimizes the seismic path through it, and hence the corresponding anelastic attenuation. Regarding Hawaiian stations, we have discussed in *Talandier and Okal* [1997] the role of the steep underwater cliffs (presumed to be the heads of fresh basaltic lava flows) documented in the immediate vicinity of the southeastern shore of the Big Island, in controlling an efficient seismic-to-acoustic conversion upon generation of *T* waves from Hawaiian earthquakes. The case of the Bolivian *T* phases is conceptually the exact conjugate, where source and receiver are exchanged. The small island of Mehetia, on which MEH is located, is a very steep, young and unconsolidated edifice, whose underwater bathymetry also features steep slopes reaching 45°.

In the case of larger island edifices, such as Upolu (AFI) or the Gambier Islands (RKT), a significant land path is traveled at seismic velocities after the acoustic-to-seismic conversion, and an appropriate correction to the arrival time of the *T* phase must be effected. In *Talandier and Okal* [1997], we have documented the nature of the seismic wave generated at the conversion, as a function of the geometry of the island and of the distance of the receiver from the converting shore. In the presence of a steep slope, and provided the station lies beyond a shadow zone of about 8 km length, the *T* wave is converted into a *P* wave, and the

correction is obtained readily from an appropriate crustal model. At shorter distances, and/or in the absence of a steep slope, an *S* wave or a guided surface wave is generated. Similar conclusions were reached by *Piserchia et al.* [1997], using a finite difference code to model the acoustic-seismic conversion.

Table 1 lists in its rightmost columns the arrival times of the maximum of the *T* phase at the stations, corrected when necessary for on-land travel.

#### Scattering by Islands Close to the Receiver

At a number of stations, complexity in the record of the *T* phase suggests that acoustic energy is being absorbed by an island or seamount structure located in the path of the *T* wave, and converted into seismic waves which are then scattered ahead of the *T* wave. Depending on the relative size of the scatterer and the receiver island, the signal may consist of (1) a small crustal phase precursory to the main *T* phase (while no such examples were documented from the Bolivian earthquake, we have observed instances of scattering of *P* waves by the small island of Tetiaroa in the Society Islands); (2) splitting of the *T* wave record (scattered wave and remnant of *T* wave having similar amplitudes; Bolivian *T* waves at Niue, scattered by Beveridge Seamount); or (3) a *T* phase arriving faster than expected (masking by an island as big as or larger than the receiving island; Bolivian *T* waves at Rarotonga, masked by Mangaia).

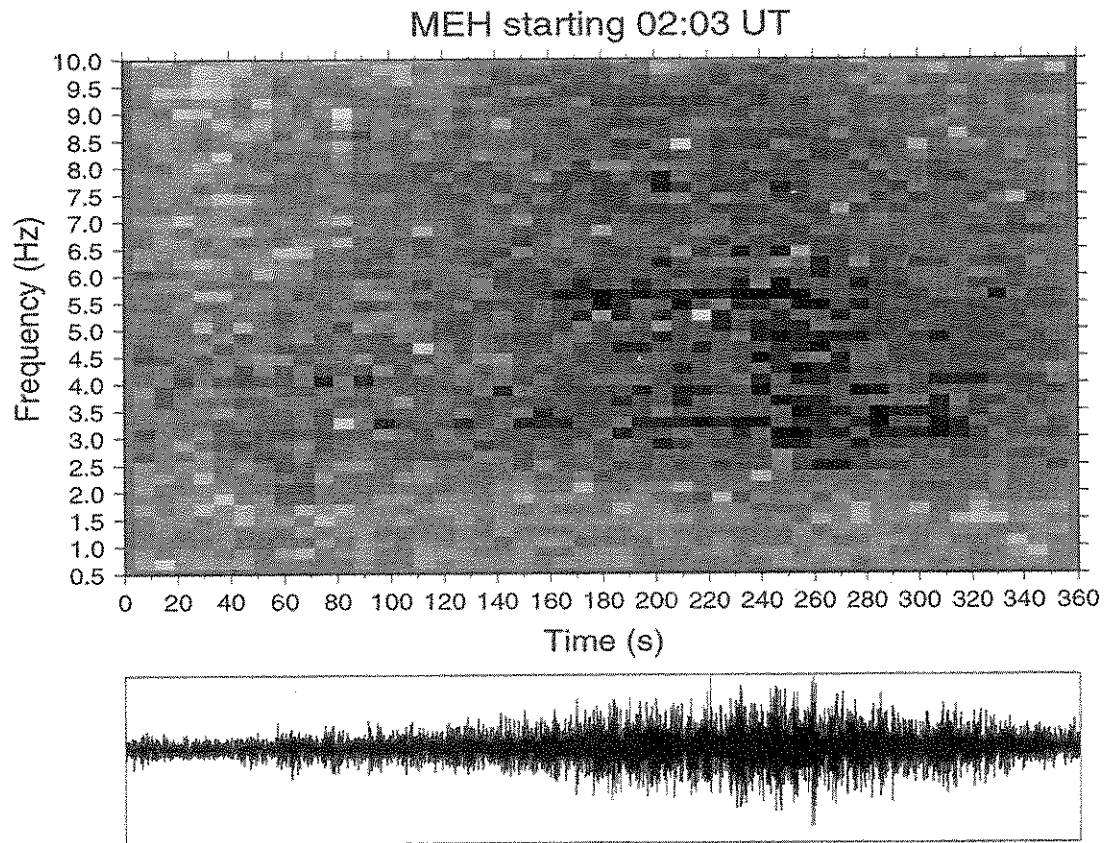


**Figure 2.** (top) Spectrogram and (bottom) seismogram of the *T* phase at MEH (Mehetia, French Polynesia). The seismogram (which can be taken as representative of ground velocity) was Fourier-analyzed over moving windows of 10.24 s duration. The spectrogram represents the logarithm of the resulting spectral amplitude as a function of time and frequency, interpolated at steps of 7.5 s in time and 0.2 Hz in frequency. Darker shades correspond to larger spectral amplitudes.

## Modeling

We investigate systematically the generation of the *T* waves recorded at all the stations in the dataset in the following way: We assume that the seismic-to-acoustic conversion takes place along the coast of South America, at a depth typical of the SOFAR channel. We use a map of the 1000-m isobath, digitized from 5°N to 30°S at ~30 km interval, and later refined to a shorter step (~5 km) from 15°S to 23°S. We consider each point as a possible conversion site and compute the travel time of the *T* wave from that point to the various island receivers. On the land side, we consider that the path from the source to the conversion point could be traveled as either a *P* or an *S* wave. This approach is more general than simply inverting our arrival times for the space-time location of the conversion point, since the latter would assume that all *T* phases are generated simultaneously at the same point.

Following the many detailed studies of the source of the Bolivian earthquake [Lundgren and Giardini, 1995; Wu *et al.*, 1995; Ihmlé and Jordan, 1995], we note that the time of maximum rate of release of seismic moment is about 25 s into the source, or 0033:41 UT. Figure 1 shows that this delay accurately predicts the maximum amplitude of the *P* wave at a station such as HUL. By adding this origin time for the maximum moment release to the *P* and *T* (or *S* and *T*) travel times, we obtained the predicted arrival times at

the various island stations, as a function of the location of the conversion point along the South American coast. These results are plotted on Figures 3 (*P* → *T* conversion) and 4 (*S* → *T*), in the form of the residual *r* of the observed travel time with respect to its computed value.

It is immediately clear that conversions along the great circle paths (outlined by the vertical arrows in Figures 3 and 4) would result in times much faster than observed, by an average of 275 s for *P* → *T* conversions and 175 s for *S* → *T*. While great-circle travel may explain the times of initial emergence of the *T* phase, the bulk of the energy in the *T* wave arrives later, and thus must proceed from a different conversion mechanism. This delay is particularly significant for the northern stations (WHA in Hawaii and OGS in the Bonin Islands) where it reaches 13 to 20 mn.

A second observation is that our dataset separates into two groups of stations: the southern stations, including Polynesia, Cook Islands, Niue, and Micronesia; and the northern ones, including Hawaii and Bonin Islands. The pattern of residuals are generally common within a group, but vary substantially between the two groups.

A third observation is that *P* → *T* conversions are unlikely to explain the arrival times at the various islands. While in principle, they could explain Polynesian arrivals if taking place in North Ecuador or South Colombia ( $\lambda = 3.3^\circ\text{N}$  (MEH) to  $1.6^\circ\text{N}$  (TBI and RKT)), the Hawaiian and Bonin records would require conversion around  $22.9^\circ\text{S}$ . It

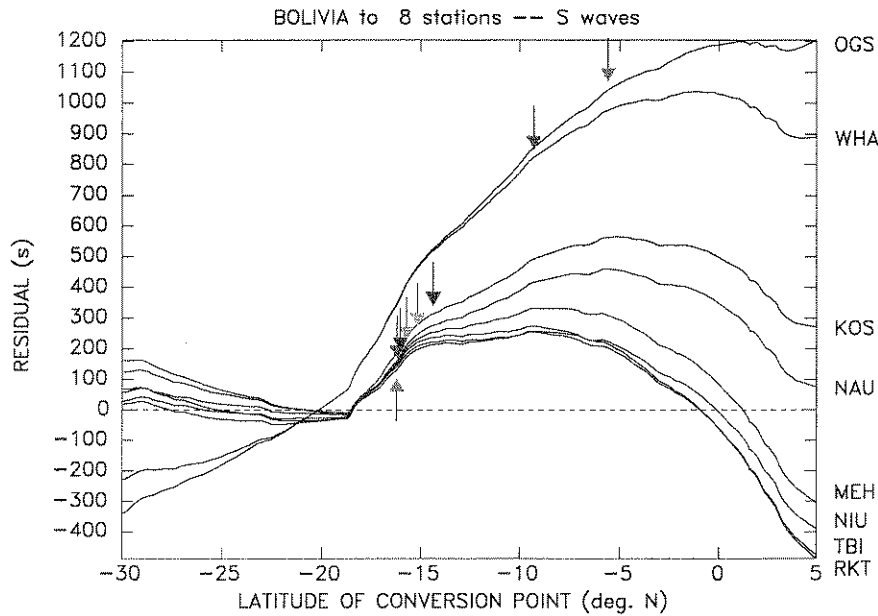


**Figure 3.** Residual (observed minus computed) travel times to the various Pacific sites plotted as a function of the latitude of the conversion point at the South American coast. Arrows refer to propagation (and conversion) along a great circle path. Land propagation from the hypocenter to the coast is modeled as a *P* wave.

would be difficult to explain why these two distant sections of the coast would be both so efficient in the radiation of *T* wave energy, and so selective in their azimuths of radiation. Furthermore, the Micronesian records (KOS, NAU) cannot be explained by *P* → *T* conversion anywhere along the South American coast.

On the other hand, we find that *S* → *T* conversion in the 18.5–20°S latitude range can explain all observations. Figure 5 is similar to Figure 4 for the finer grid of conversion points. It suggests that the southern group of *T* waves is generated around 18.5°S, 71.0°W, while the northern one (to Hawaii and Bonin) has its source at 20.0°S, 70.4°W. Although the conversion point leading to the best set of

residuals ( $\langle |r| \rangle = 4.8$  s) is at (18.53°S, 71.04°W), we actually favor the neighboring point (18.46°S, 70.96°W;  $\langle |r| \rangle = 5.0$  s) as the origin of the *T* waves for the southern group of stations. The reason is that this scatterer is located inside a curved, convex section of the 1000-m isobath. While the precise modeling of the seismic-to-acoustic conversion would require a three-dimensional analysis on a scale comparable to the wavelengths involved [Piserchia *et al.*, 1997] and hence a far more detailed knowledge of the relevant bathymetry, we note that, in general terms, the presence of a bay will focus the seismic energy and lead to greater acoustic amplitudes. At the same time, the particular shape of the 1000-m isobath, controlling the SOFAR

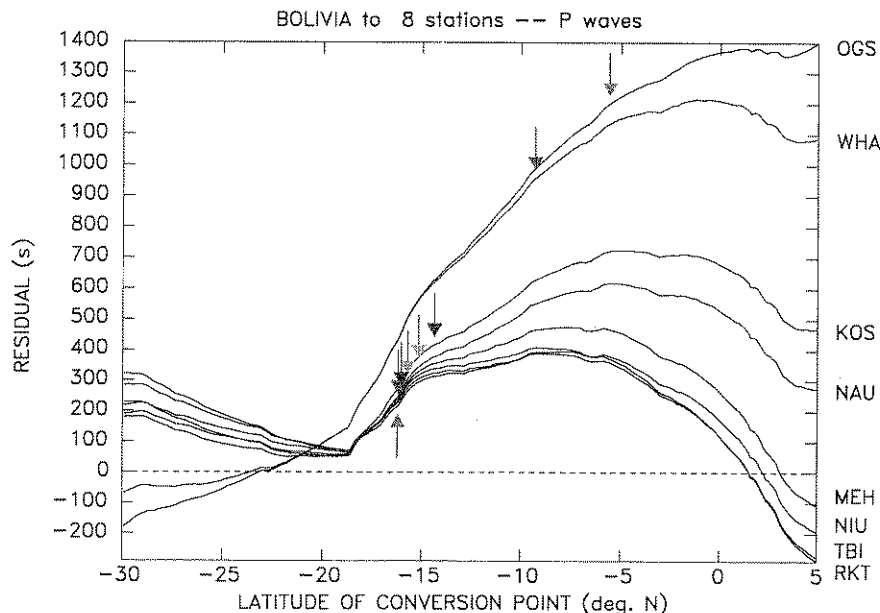


**Figure 4.** Same as Figure 3 assuming *S* wave propagation from source to conversion point.

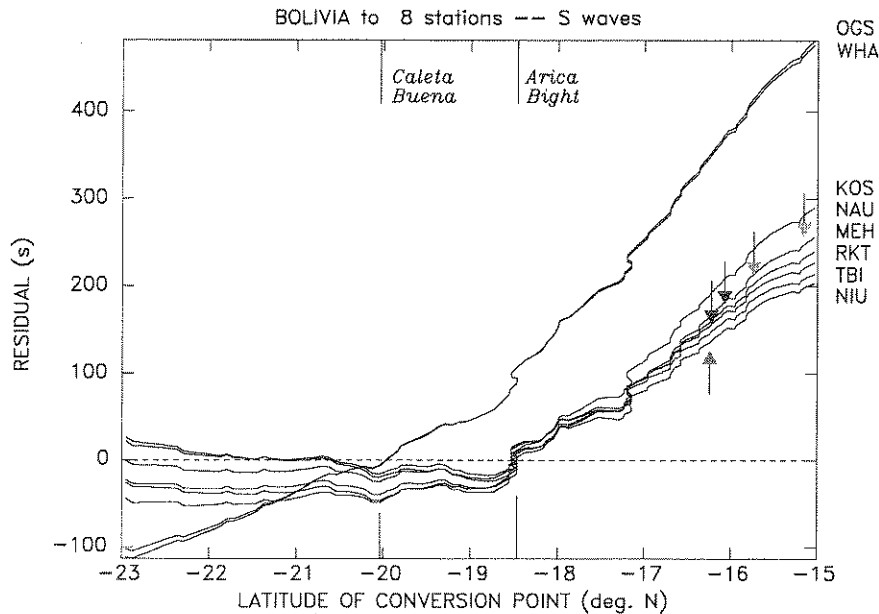


**Figure 5.** Same as Figure 4 for the finer digitization of the conversion slope. Note that all South Pacific *T* phases are accurately modeled by conversion at the Arica Bight, while OGS and WHA require conversion farther South. The vertical bars indicate the location of the preferred conversion points.

channel in the Arica Bight, will generate a shadow beyond azimuths  $265^\circ$  and prevent the generation of a *T* wave towards Hawaii and the Bonin Islands. Hence the enhanced delay observed at those stations, whose *T* waves are generated at the next favorable location down the coast, at  $20^\circ\text{S}$ .

We thus conclude that the maxima in the energy of the *T* phases received at stations scattered all across the South Pacific can be explained by assuming that a powerful source of acoustic energy was released into the SOFAR channel around  $18.46^\circ\text{S}$ ,  $70.96^\circ\text{W}$ , at 0036:41 UT. At the relevant location (the Arica Bight), this time would have corresponded to the arrival of the *S* wavetrain having left the source at the time of the maximum of moment rate release, as defined for example by the study of *Lundgren and Giardini* [1995]. On the other hand, the *P* waves would have reached the preferred point approximately 80 s earlier, which would be impossible to reconcile with the observed times for the most intense *T* phases. For the northern stations (WHA and OGS), the preferred source is at  $20.04^\circ\text{S}$ ,  $70.32^\circ\text{W}$ , near the town of Caleta Buena on the Chilean coast slightly North of Iquique, and its source time, 0036:57 UT, also corresponds to the *S* arrival. Note that it is difficult to estimate the precision of these figures. Since our method elects to associate the generation of the *T* wave with a seismic phase, we cannot have an independent resolution both in space and time; rather, we believe that the general precision of the readings on time series and spectrograms ( $\sim 5$  s) results in a precision on the order of about 30 km for the conversion point along the coast, which also happens to be our coarser digitization step.

Figure 6a summarizes in map form the generation and propagation of the *T* waves from the Bolivian earthquake. Figure 6b is a close-up of the conversion region.

### The Case of the 1970 Colombian Earthquake

We give here a brief comparative discussion of *T* wave records from the great Colombian earthquake of July 31,

1970. *T* waves were well recorded at a temporary station, which happened to be operating at the time, on the island of Reao, at the extreme end of the North Tuamotu group ( $18.5^\circ\text{S}$ ,  $136.4^\circ\text{W}$ ). This remarkable record, a detail of which is shown on Figure 7, was written at fast paper speed (5 mm/s), allowing hand digitization of the *T* phase and processing by spectrogram analysis (Figure 8). On the other hand, the Colombian *T* wave at RKT barely emerges from the noise on the standard short-period channel (using the same gain as in 1994; the *T*-wave channel was not developed in 1970), indicating an amplitude several times smaller than for the Bolivian event, and preventing its use for the precise determination of an arrival time.

A search of records from the World-Wide Standardized Seismological Network (WWSSN) failed to yield any evidence of a *T* phase, not a surprising result given both the generally poor operating magnifications of short-period WWSSN oceanic stations, and the lower amplitude of the Colombian *T* waves. Thus, we are left with a single arrival time measurement, that for the maximum of *T* energy at Reao, at 1820:06 UT. Figure 9 investigates the site of the seismic-to-acoustic conversion for that single datum, using a hypocentral origin time of 1708:06 UT, and a delay of 40 s for the maximum of moment release [*Gilbert and Dziewonski*, 1975]. We find that the Reao arrival is perfectly explained by conversion of a *P* wave at the point ( $4.6^\circ\text{S}$ ,  $81.4^\circ\text{W}$ ) where the great circle to the station crosses the Pacific shoreline, at Punta Pariñas, Perú, the westernmost end of South America. On the other hand, conversions from *S* waves would result in wavetrains delayed significantly, by at least 100 s. This is a major difference with the case of the Bolivian earthquake.

### Inferences on Regional Propagation in the Andes

Having established the epicenter and origin time of trans-Pacific *T* waves from the Bolivian earthquake, there

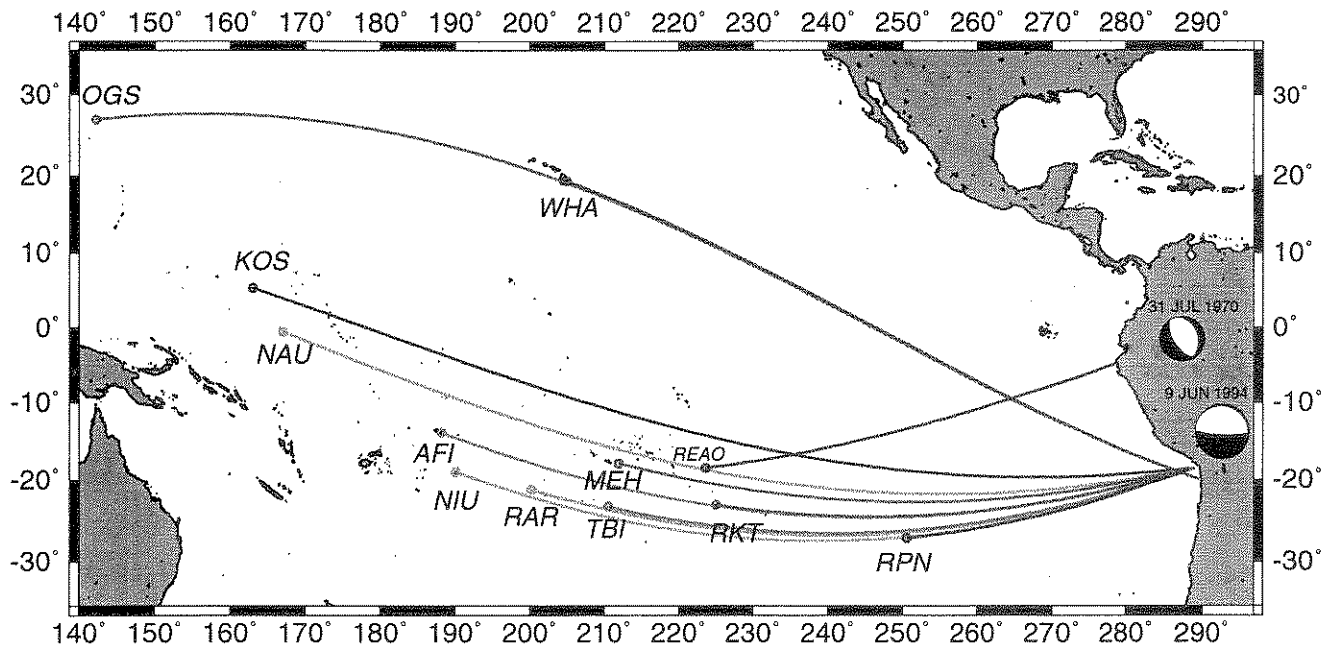


Figure 6a. Map of the Bolivian *T* paths to receiving stations in the Pacific. Also shown is the Reao path from the Colombian event (smaller symbol).

remains to understand the process of their generation. Ultimately, the conversion of seismic waves to acoustic energy is controlled by the fine bathymetry of the South American coast, on a scale comparable to the wavelengths involved, or a few hundred meters. In the absence of its precise

knowledge, we will focus on the origin of the high-frequency seismic energy available for conversion.

In order to verify that intense high-frequency *S* waves were indeed received at the Arica Bight during the 1994 Bolivian earthquake, we searched for regional records of the

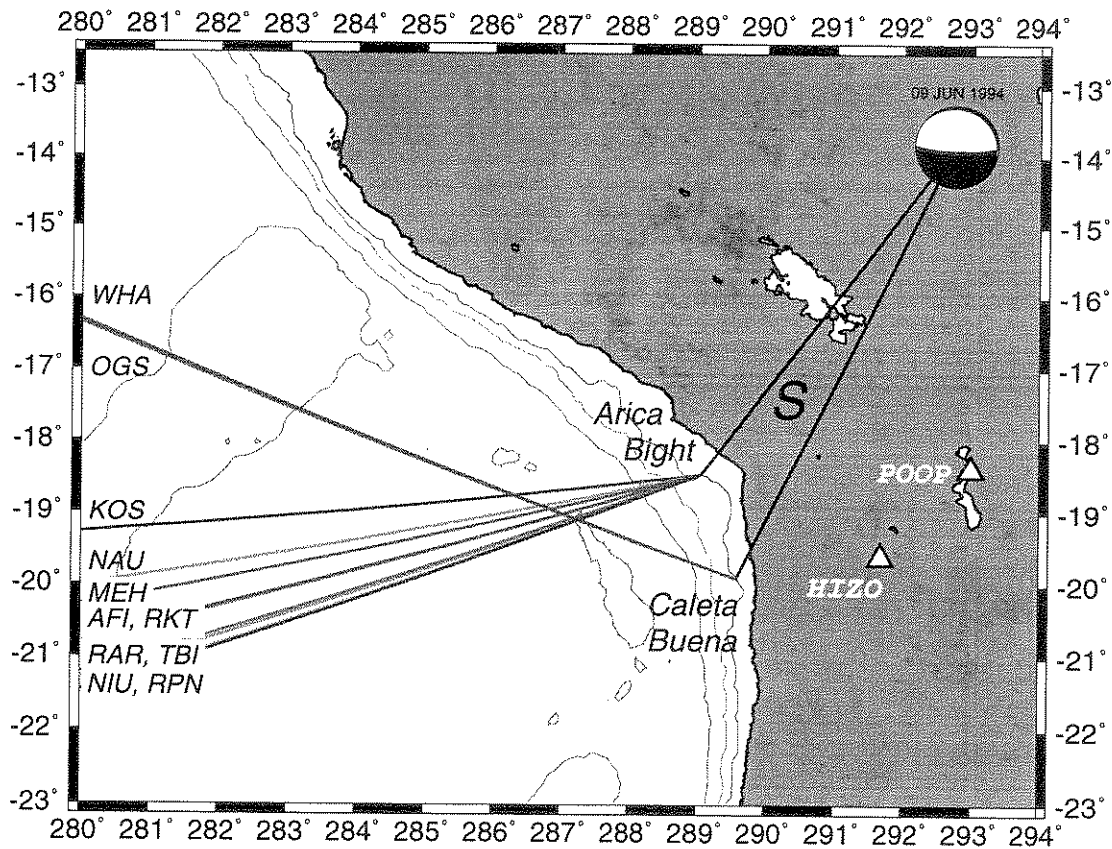
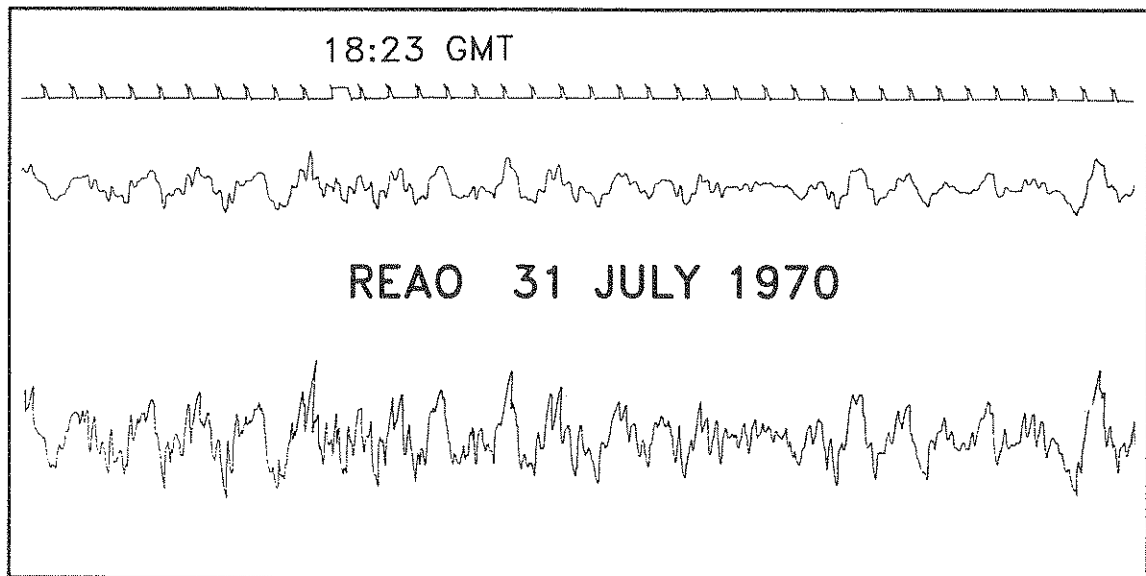


Figure 6b. Close-up of Figure 6a, detailing the generation of *T* waves at the South American coast. Iso-baths shown are 1000, 2000, and 4000 m. Note curvature of the 1000 m line at the Arica Bight. Also shown (triangles) are BANJO/SEDA stations POOP and HIZO.





**Figure 7.** Close-up of the record of the 1970 Colombian event at Reao. The two traces correspond to two different gains of a standard short-period instrument. Tick marks at the top are seconds. The *T* wave is the fast oscillation prominently seen on the lower trace.

event. Unfortunately, we could not identify any seismic station in the vicinity of Arica or Iquique, which would have been operating at the time. While the earthquake was reported felt over most of North Chile, such reports are generally too vague to provide insight into the propagation of individual waves in the absence of instrumental data.

To the best of our knowledge, the stations closest to the conversion point were the portable receivers of the BANJO/SEDA project [Beck *et al.*, 1994]. Even so, the closest available station, HIZO, is still 225 km from the shoreline near the Caleta Buena conversion point, and 317 km from the Arica one. In addition, the *P* and *S* records of

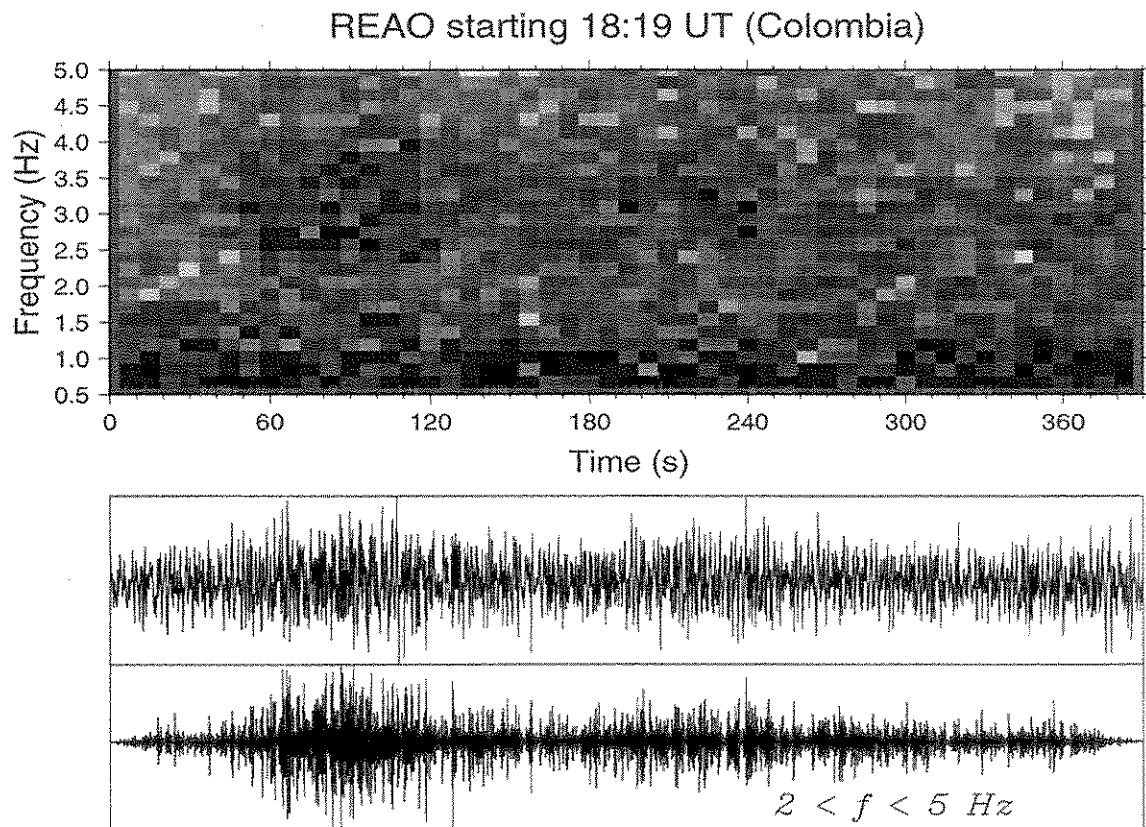


**Figure 8.** (top) Spectrogram of the Reao *T* phase from the 1970 Colombian event. (bottom) Time series at Reao plotted from the full digitized record (Figure 7). A filtered trace is also shown, on which the *T* phase is clearly identified.



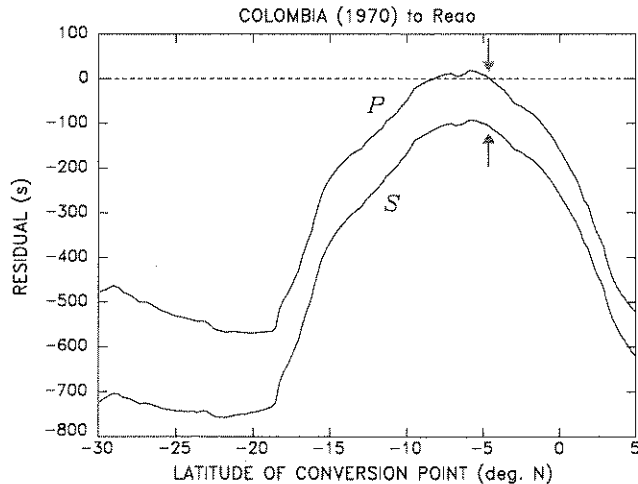


**Figure 9.** Same as Figures 3 and 4 for the single Reao record of the 1970 Colombian earthquake. Note perfect agreement with  $P \rightarrow T$  conversion at the great circle crossing point.

the great Bolivian earthquake saturated at most stations, and thus, we elected to study the  $P$  and  $S$  phases of the second large aftershock of the event (June 9, 1994; 0930 UT), located by the US Geological Survey only 28 km from the main event (the first aftershock, at 0115:18 UT was 102 km from the main shock). We selected stations POOP and HIZO, whose records are shown on Figure 10. POOP is located on the Altiplano, whereas HIZO is on the Western Cordillera, and can be presumed to best replicate the geometry of the rays from the hypocenter to the Arica Bight and Caleta Buena. It is immediately apparent that the  $S$  waves at HIZO are stronger and of significantly higher frequency than at POOP, even though the epicentral distance is larger. We further investigated this property in the Fourier domain by comparing the ratios of the spectral amplitudes  $X_S(\omega)/X_P(\omega)$  at both stations, the  $S$  wave train being analyzed on both horizontal components (Figure 11). The decay of this ratio with frequency is clearly faster at POOP

than at HIZO. If interpreted as entirely due to shear anelastic attenuation, it requires  $Q_\mu \approx 850$  at HIZO and 400 at POOP. An important consequence of the high whole-path  $Q$  value to HIZO is that the low-attenuation material, i.e., the cold slab, is most likely continuous along the path of the  $S$  wave. This provides supporting evidence for the mechanical continuity of the slab under South America, which has been inferred from a variety of observations, such as seismic tomography [Engdahl *et al.*, 1995] and the coherence of focal mechanisms of earthquakes deeper than the seismic gap [Kirby *et al.*, 1995].

Our observations are also reminiscent of those of Sacks [1969] and Isacks and Barazangi [1973], although they were limited to lower frequencies ( $f \leq 2$  Hz) by their use of analog WWSSN seismograms. Our geometry is perhaps closest to that of James and Snoke [1990], who showed that the slab could channel  $P$  waves from deep Peruvian sources to CUS (Cuzco, Perú), resulting in a second " $P$ ," arrival following direct  $P$  by 1 to 3 s, of higher frequency content due to lower attenuation in the colder slab material, and often of larger amplitude, than direct  $P$ . On Figure 12, we present cross sections taken along the great circle planes from the hypocenter of the Bolivian earthquake to the conversion points at Arica and Caleta Buena. The asterisks on these figures represent the position of seismically active segments of the slab, as contoured by Cahill and Isacks [1992]. The dotted lines represent the paths of the direct  $P$  arrivals, as computed using James and Snoke's [1990] crust and upper mantle model. They would also be the paths of direct  $S$  waves, assuming that the Poisson ratio of the material is constant. We show as solid lines the proposed paths of the channeled  $S_r$  waves, obtained by assuming that they first propagate to the extremity of the active slab, undergo some sort of reflection in the manner of James and Snoke's [1990]  $P_r$ , and then propagate to the conversion point. Note that in both instances, the latter propagation is largely confined to the seismic zone, and hence to the cold, low-attenuating slab. These models are extremely crude, since they do not take into account the unknown geometry of the slab in the seismic gap, and they make the simplifying assumption of propagation in the great circle plane. How-

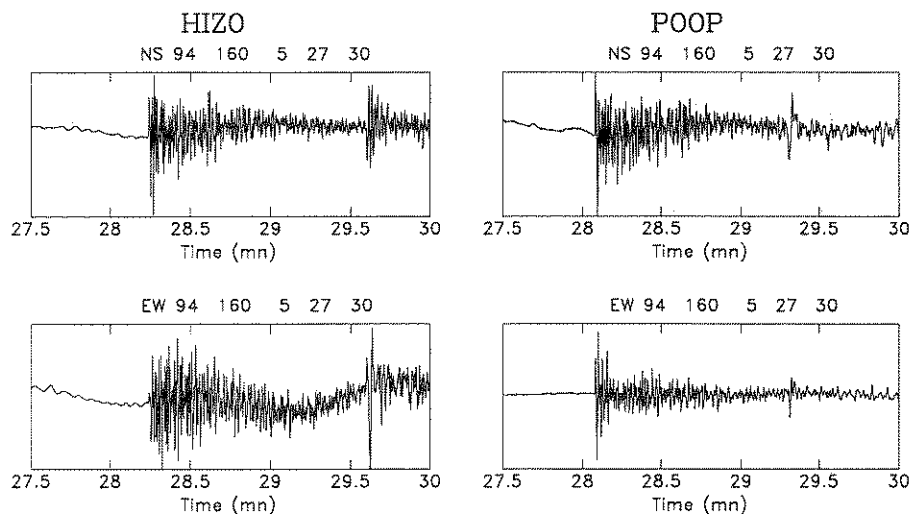


**Figure 10.** Horizontal seismograms of the 0526 UT aftershock of the Bolivian earthquake at temporary stations HIZO (left) and POOP (right; see map on Figure 6b). Note higher frequency character of  $S$  wave at HIZO and generally larger amplitude, as compared to POOP.

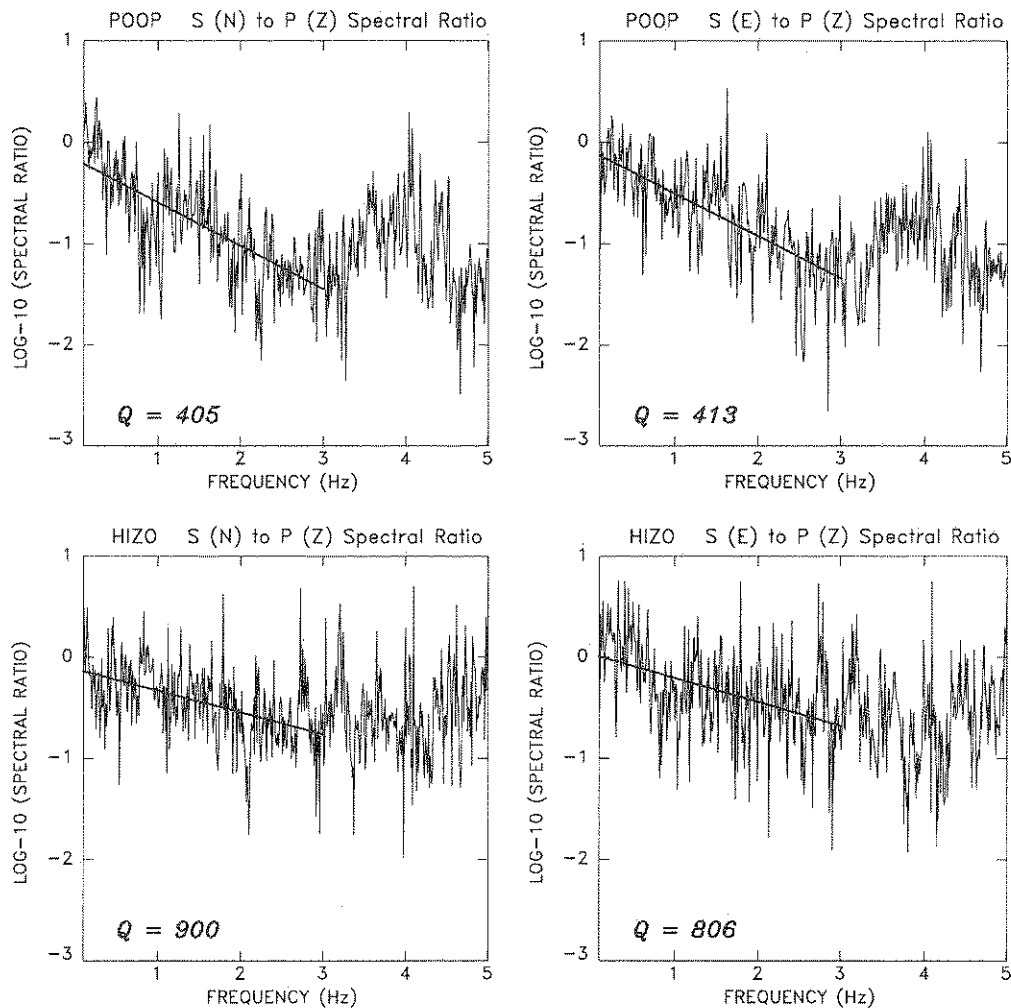


**Figure 11.** *S*-to-*P* spectral ratios at HIZO and POOP. Note the lower attenuation at HIZO.  $Q_{\mu}$  values are obtained by modeling the *S*/*P* decay between 0.1 and 3 Hz. The POOP spectra are affected by background noise at higher frequencies.

ever, they suggest that a favorable geometry for reflection and channeling may indeed exist. The deflection angle between the two parts of the ray at the tip of the Wadati-Benioff Zone is computed to be  $28^{\circ}$  in the case of the Arica ray (respectively  $25^{\circ}$  for Caleta Buena). This in turn would correspond to reflections at an incidence of  $76^{\circ}$  (respectively  $77^{\circ}$ ), for which a velocity contrast of 3% (respectively 2.5%) would be sufficient for post-criticality and hence total reflection. This level of velocity contrast is well within the range suggested both by tomographic imaging [Engdahl *et al.*, 1995] and thermo-mineralogical models of the downgoing slab [Helffrich *et al.*, 1989]. Finally, the focal geometry of the Bolivian earthquake predicts larger *SV* radiation coefficients up the slab ( $R^{SV} = 0.60$ ) than for direct *S* (-0.14; respectively 0.48 and -0.33). While *P<sub>r</sub>* waves are also expected to be strong ( $R^P = -0.58$ ; respectively -0.78), we propose that the prominence of the *S*  $\rightarrow$  *T* conversion is the combined result of the larger excitation of the *S* wave (by a factor  $\alpha^3/\beta^3 \approx 5$ ), the favorable radiation patterns, the exceptionally low *S* attenuation in the slab, and a geometry of the converting slope that, in the absence of knowledge of its fine bathymetry, we must assume is particularly favorable to *S* waves. Note finally that the delay in propagation of *S<sub>r</sub>* with respect to direct *S* would be expected to be about 1.7

times that of *P<sub>r</sub>* with respect to direct *P*, or between 2 and 5 s, based on the observations of James and Snoke [1990]. This figure would not affect our modeling significantly, given the precision of our *T* wave picks.

Finally, in the case of the 1970 Colombian earthquake, we note that the tomographic results of Engdahl *et al.* [1995] in the 200–400 km depth range do not reveal a continuous slab in North Peru–South Colombia, as they do in South Peru–North Bolivia; if their resolution is comparable for the two regions, the inference would then be that a high-frequency *S* wave from the Colombian source would stand little chance of reaching the surface with a vigorous amplitude. Furthermore, the direct ray towards Punta Pariñas practically coincides with the tensional axis ( $R^P = 0.98$ ), all this evidence supporting our observation of a *P*  $\rightarrow$  *T* conversion.

## Conclusions

1. The 1994 Bolivian earthquake generated very prominent *T* phases throughout the Pacific Basin. Their amplitude was at least several times larger than for the 1970 Colombian earthquake, based on the direct comparison of records written on the same instrument at Rikitea.

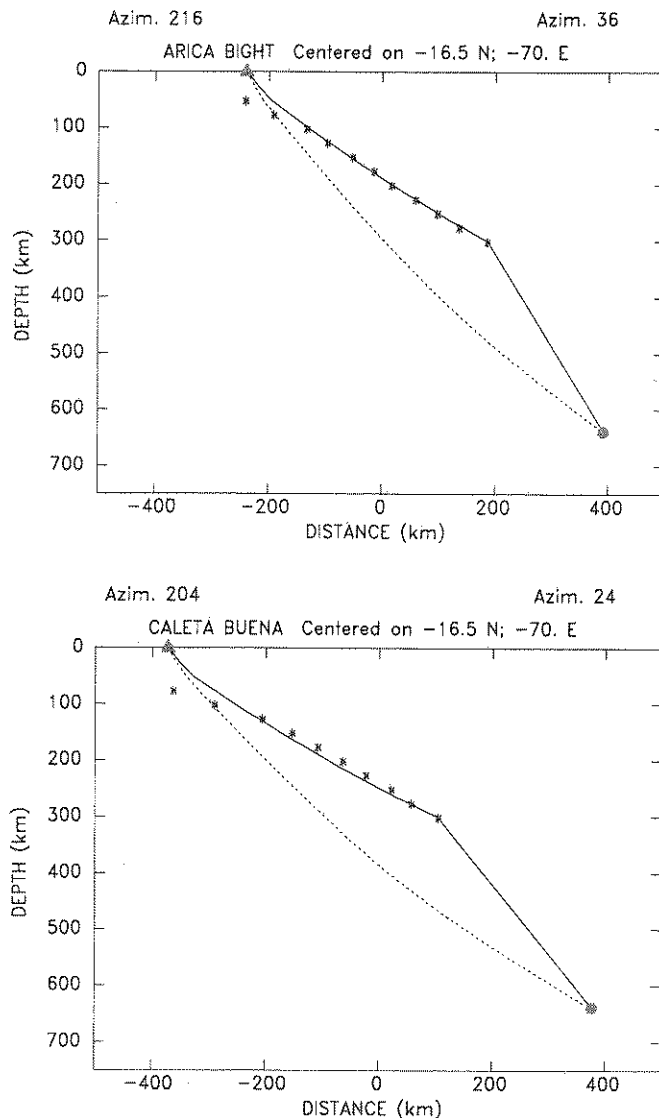


**Figure 12.** Possible model of the channeling of high-frequency *S* energy from the hypocenter of the Bolivian earthquake to the conversion points at (top) Arica and (bottom) Caleta Buena. See text for details of the ray tracing.

2. The Bolivian *T* waves were received as far as the Bonin Islands. However, in at least one instance (RPN), they could not be extracted from the record, probably due to scattering and attenuation along the Sala-y-Gomez Seamount chain. In other instances, scattering in the vicinity of the

receiver resulted in splitting of the arrival, with a seismic wave preceding (NIU) or replacing (RAR) the regular *T* wave.

3. The arrival times of the maximum of the energy in the *T* phase are systematically incompatible with direct propagation and conversion along the great circle from the epicenter to the receiver island. This a major difference with the case of the 1970 Colombian event.

4. Travel times to stations in the South Pacific require generation of the *T* wave at the Arica Bight, upon arrival of the regional *S* wave from the episode of maximum moment release in the source, as defined by several independent studies of the source of the Bolivian earthquake. Stations in the North Pacific (Hawaii, Bonin Islands) are masked from that location by the local structure of the Arica Bight, and their *T* waves are generated farther South, at approximately 20°S, once again upon arrival of the regional *S* wave.

5. The analysis of records from the BANJO/SEDA experiment confirms that high-frequency *S* waves are recorded preferentially at a station close to the South American coast, while they are absent from a station located further inland. Such waves can be preserved during propagation from a deep source only if they travel a low-attenuating path.

6. The proposed model for the generation of the Bolivian *T* phases has an *S* wave channeled along the slab from the hypocenter to the conversion point. Thus the slab needs continuity in its mechanical properties (and in particular in its low attenuation) in a region where the seismic Wadati-Benioff Zone is interrupted from 300 to 600 km. In this respect, our results bring support to the inference obtained from seismic tomography for a continuous slab in that part of central South America. The weaker character of the 1970 Colombian *T* waves and their different travel characteristics may be ascribed (at least in part) to the possibility that the slab is actually mechanically discontinuous under Colombia.

## Appendix: Description of Individual Records

### Hawaii

The record at station WHA is described in the main text; since the station is less than 1 km from the seashore, no correction is used.

### French Polynesia

Figure A1 shows the *T* arrival at RKT (Rikitea, Gambier), both on the regular short-period channel and on the special "*T*-wave channel", which it saturates, indicating amplitudes in excess of 0.03  $\mu\text{m}$  peak-to-peak. No digital

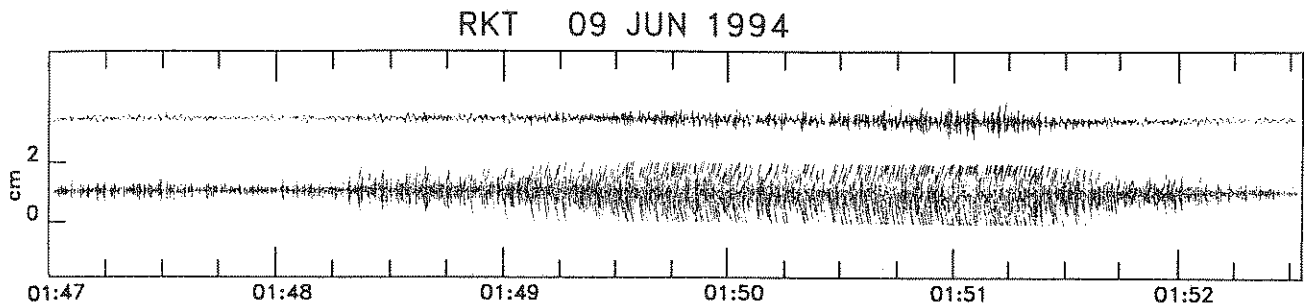


**Figure A1.** Original record of the Bolivian *T* phase at RKT (Rikitea, Gambier Islands). (top) Regular short-period channel (gain 125,000 at 1 Hz). (bottom) "*T*-wave" channel (gain  $2 \times 10^6$  at 3 Hz). Note that the latter is saturated.

record is available. The *T* phase emerges from background noise around 0148:15 UT and the maximum amplitude is registered at 0151:04. Our previous study [Talandier and Okal, 1997] indicates a station correction of 5 s to account for the 12-km path across the Gambier lagoon.

Similar determinations were made at MEH and TBI, with arrival times of the most intense *T* phase listed in Table 1. No correction was used at Mehetia, given the very small size of the island. Tubuai is a volcanic island of the Austral chain, fringed by a large lagoon and reef. We estimate that the station is 10 km from the conversion point and use a correction of 4 s. Peak-to-peak amplitude at TBI reached 0.01  $\mu\text{m}$ .

#### Other permanent stations: IRIS sites

**Station AFI, Upolu, Western Samoa.** Upolu is a reefed shield volcano aged 1–3 Ma, and as such, conversion to *P* phases should be expected. The spectrogram of the *T* phase at AFI, shown on Figure A2, is remarkable in that it features several maxima, which could suggest a multipathed *T* wave. However, several of these signals (e.g., at 0251 UT) correspond to local earthquakes, which can be located from records of the Southwest Pacific array. In particular, the most prominent signal, between 0235 and 0240, is generally too rich in low frequencies to be interpreted as a teleseismic *T* phase, and rather exhibits the perfect  $P_o$ ,  $S_o$ , *T* signature of an earthquake at a distance of 400 km (in the terminology of Walker [1984]). The *T* wave from the Bolivian earthquake would be expected exactly at the time of  $S_o$ , and we cannot rule out that it is obscured by the regional earthquake. Consequently, we cannot use this signal in our modeling.

**Station RPN, Easter Island.** As shown on the spectrogram presented on Figure A3, we were unable to recognize any *T* wave at RPN, even though its response is identical to

those of other IRIS stations. This result was confirmed through both filtering of the record, and the systematic study of its spectrum. A very weak signal appears around 0112:42 UT, or 462 s into the spectrogram. This is a double arrival ( $\delta t = 1.3$  s), which could correspond to *S* and *P* conversions from an acoustic wave. However, its timing is about 590 s early; furthermore, the signal does not have the distinctive spindle shape of a distant *T* phase. Finally, a faint signal is observed about 32 s after the expected arrival; this delay and its short duration argue against interpreting it as the expected *T* phase.

This situation is intriguing, since, at only 4036 km from the Arica Bight, RPN is by far the station closest to South America, and the azimuth from the conversion point to the station is practically equivalent to that to TBI and NIU, where the amplitude of *T* waves is generous. One likely explanation is that RPN is masked from the source by the chain of Sala-y-Gomez Island and associated seamounts, which protrude into the SOFAR channel and may act to reflect and scatter the energy in the *T* wave before it reaches Easter Island (we verified that the path to RPN from the assumed source of *T* waves intersects several seamounts, while that to TBI is slightly to the North of the chain). Another hypothesis would be that Easter Island (which lacks a coral reef) does not feature, on its Eastern side, the steep underwater slopes necessary for the efficient conversion of *T* wave energy into a *P* wave capable of traveling across the island [Talandier and Okal, 1997]. However, we have verified that RPN did indeed record *T* waves following other Pacific rim events, and this explanation is unlikely.

**Station RAR, Rarotonga, Cook Islands.** The record at RAR exhibits a singularity in that the *T* phase is recorded at 0217:57, about 95 s earlier than would be expected from the common source of *T* waves at the Arica Bight, which fits other arrivals in the South Pacific (Figure A-4). In addition,

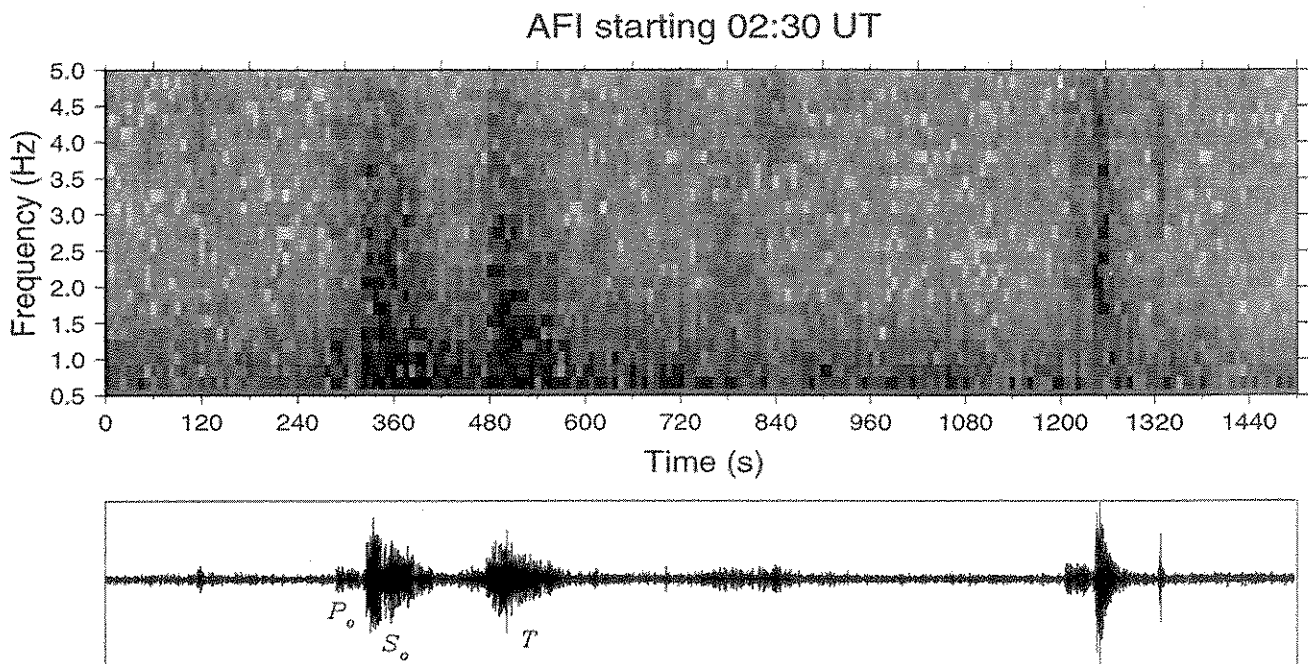


**Figure A2.** Same as Figure 2 for Station AFI (Afiamalu, Upolu). Note that the various phases are most likely associated with local seismicity.

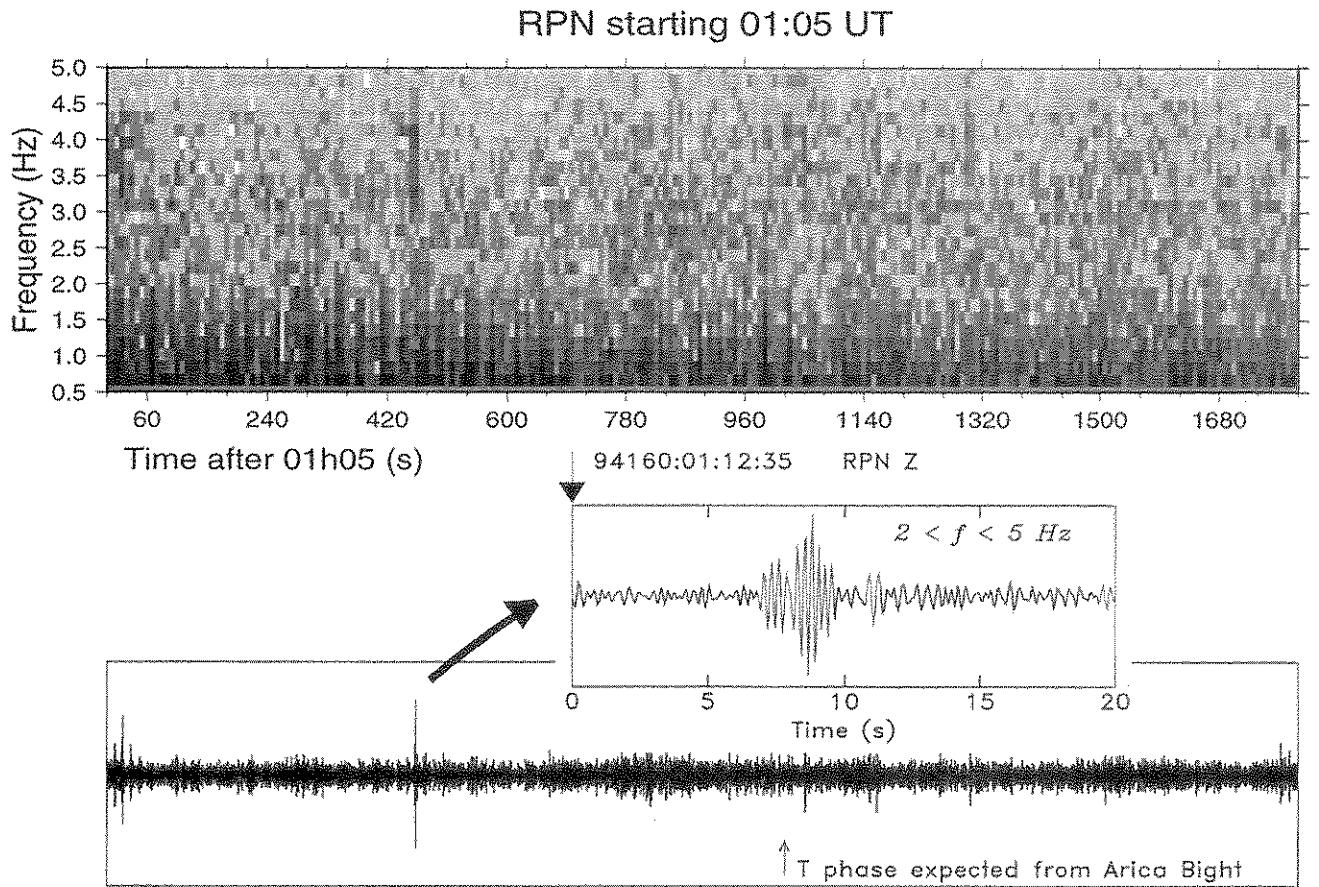


**Figure A3.** Same as Figure 2 for Station RPN (Easter Island). Note that the only substantial signal in the 3–4 Hz range (inset) does not exhibit the characteristic shape of a teleseismic *T* phase.

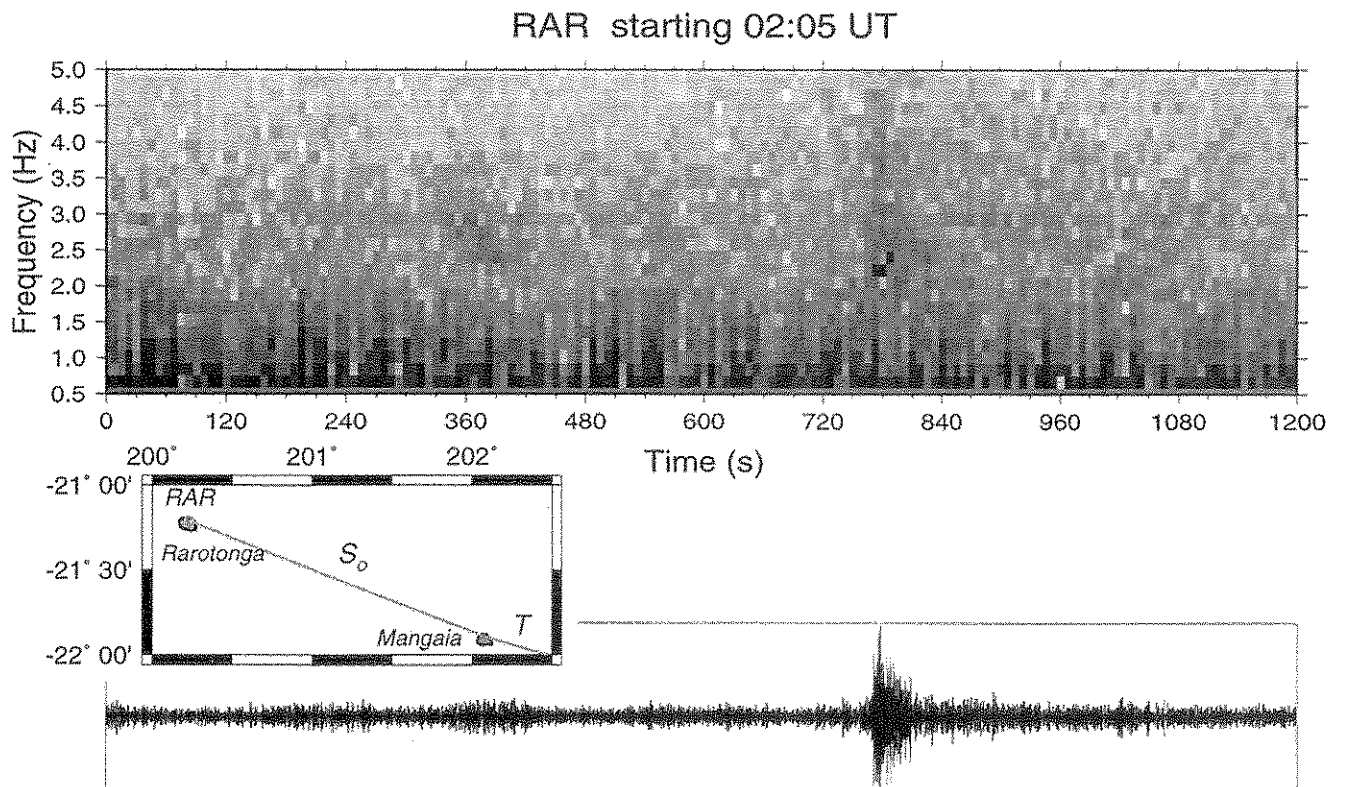


**Figure A4.** Same as Figure 2 for Station RAR (Rarotonga, Cook Islands). Inset shows the geometry of the scattering by Mangaia.

the *T* signal is very weak. This situation is not simply explained since RAR is practically on the same great circle from the conversion point as TBI, and so this advance in group time at RAR must be ascribed to a local process occurring between TBI and RAR.

We propose that the island of Mangaia (21.9°S, 157.9°W; 210 km ESE of Rarotonga) may act as a mask, which absorbs the *T* wave energy, and scatters it as a seismic wave propagating to RAR through the solid Earth structure. Similar situations are observed in Polynesia, where the small island of Tetiaroa can generate *P* wave precursors to *T* phases recorded from the North. Mangaia is only 15 km from the great circle from Arica to RAR, which we regard as being within the range of lateral uncertainties in the path of the *T* wave. The timing of the *T* phase at RAR can be explained only through propagation as an *S* wave between Mangaia and Rarotonga. Efficient propagation of high frequency oceanic upper mantle phases ( $P_o$  and  $S_o$ ) has long been documented [Walker, 1977; Talandier and Bouchon, 1979] and modeled [Mallick and Frazer, 1990], but it remains unclear why the bulk of the *T* wave hitting Mangaia would convert to  $S_o$  rather than  $P_o$ . Mangaia is an unusual island, featuring exceptionally old exposed volcanics [Turner and Jarrard, 1982], and an uplifted limestone ring, with a small recent fringing reef [Yonekura et al., 1988]. The exact morphology of the slope of the island structure and its effect on the acoustic-to-seismic conversion remain speculative. For this reason, it is not possible to assign a precise correction to the observed arrival time at RAR, and we do not use it in our modeling.

#### Other Permanent Stations: POSEIDON

We use the record at Chichi-jima, Bonin (Ogasawara) Islands (OGS). The *T* wave is prominent in the filtered record, with a typical emergent shape. The spectrogram (Figure A5) confirms that the energy is in the frequency band characteristic of *T* waves. The arrival time for the

maximum of the phase is taken as 0343:30 UT. The station is about 3 km from the shore line of Chichi-jima, a small member of the Bonin volcanic arc, which lacks a coral ring. We do not use a station correction for OGS.

#### Portable stations: Micronesia

We use records at two stations of the PASSCAL Micronesian project [Richardson and Okal, 1996]: KOS (Kosrae) and NAU (Nauru). At KOS, the *T* phase is very prominent in the spectrogram, with a maximum in amplitude at 0313:45 UT (Figure A6a). Station KOS is less than 4 km from the coastal reef, and we do not use a correction. At NAU, the spectrogram is somewhat fainter (Figure A6b), but the arrival remains clear with a maximum at 0306:30 UT. Similarly, the station is no more than 3 km from the reef, and no correction is necessary.

#### Portable stations: Niue Island

We obtained records from the 1993-1995 Southwest Pacific PASSCAL experiment [Wiens et al., 1994]. Only Niue (NIU) has a *T* phase readable in a strongly high-pass-filtered record. Unlike many high-frequency arrivals at Niue that day, this phase has both the characteristic emergence typical of *T* waves and no energy above noise level in the 1-2 Hz frequency band. This sets it apart from the more prominent signals from local earthquakes (see Figure A7). Furthermore, it features two distinct maxima at 0229:45 and 0231:36 UT, the second one being of stronger amplitude. We show in the main text that the second arrival is compatible with the times at station TBI, at a similar azimuth. We believe that the earlier arrival represents scattering by Beveridge Seamount, a large structure located 257 km ESE of Niue, in the path of the incident *T* wave. The seamount (20.0°S, 167.75°W) features a free air gravity anomaly of  $\sim 1.5 \times 10^{-3} \text{ m/s}^2$  [Sandwell and Smith, 1997] and is documented in recent bathymetric maps [Mammerickx, 1992].

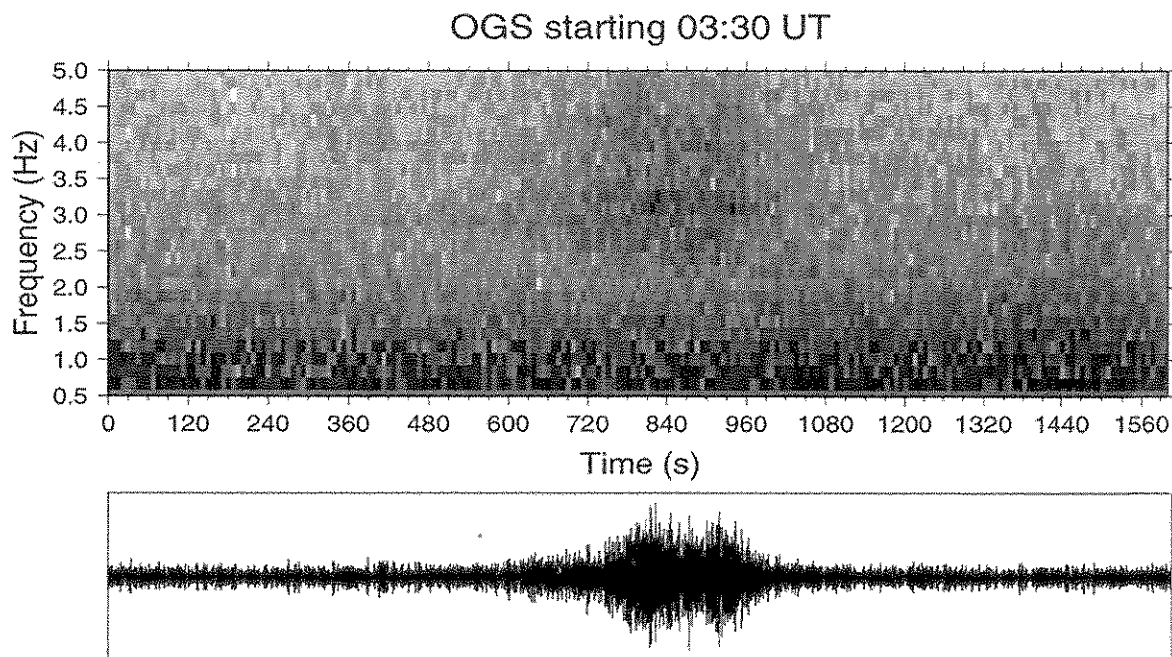


Figure A5. Same as Figure 2 for Station OGS (Chichi-jima, Bonin Islands).



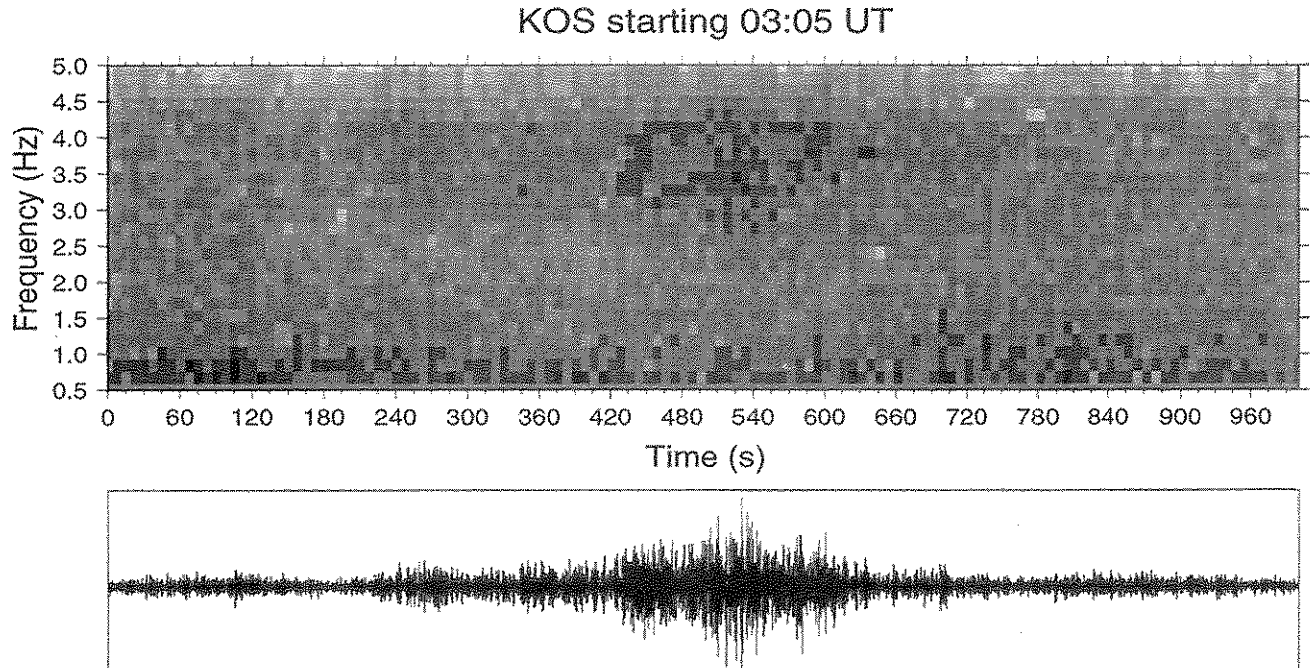


Figure A6a. Same as Figure 2 for Station KOS (Kosrae, Caroline Islands)

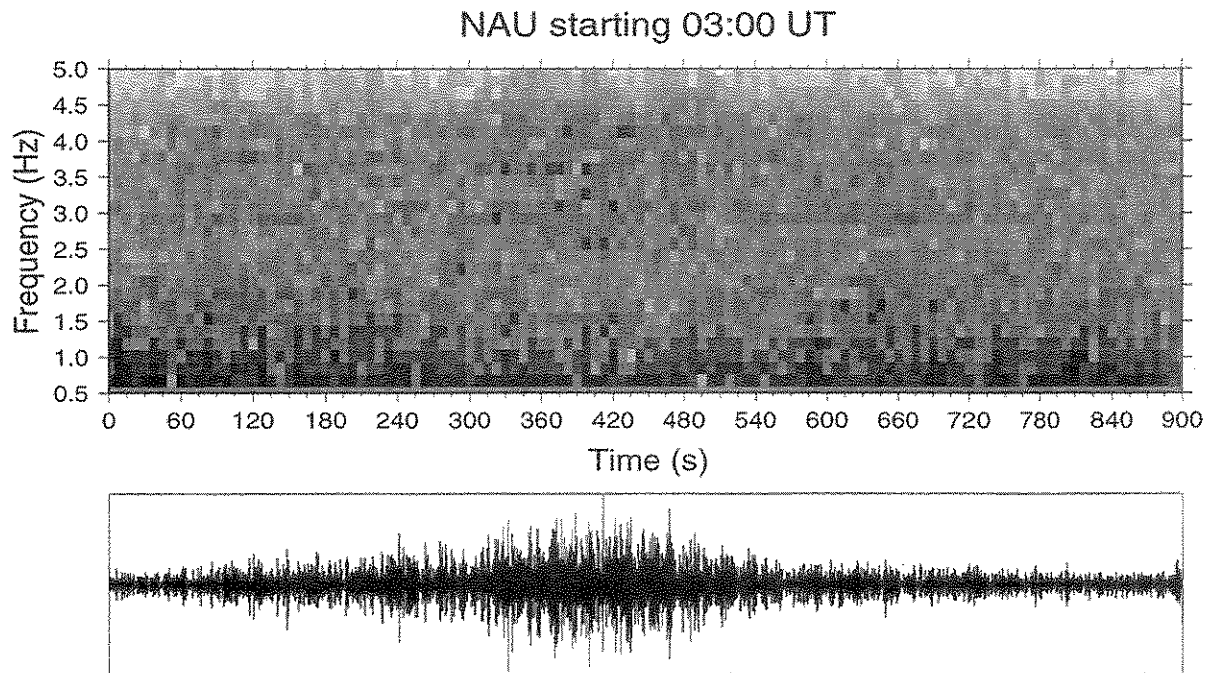
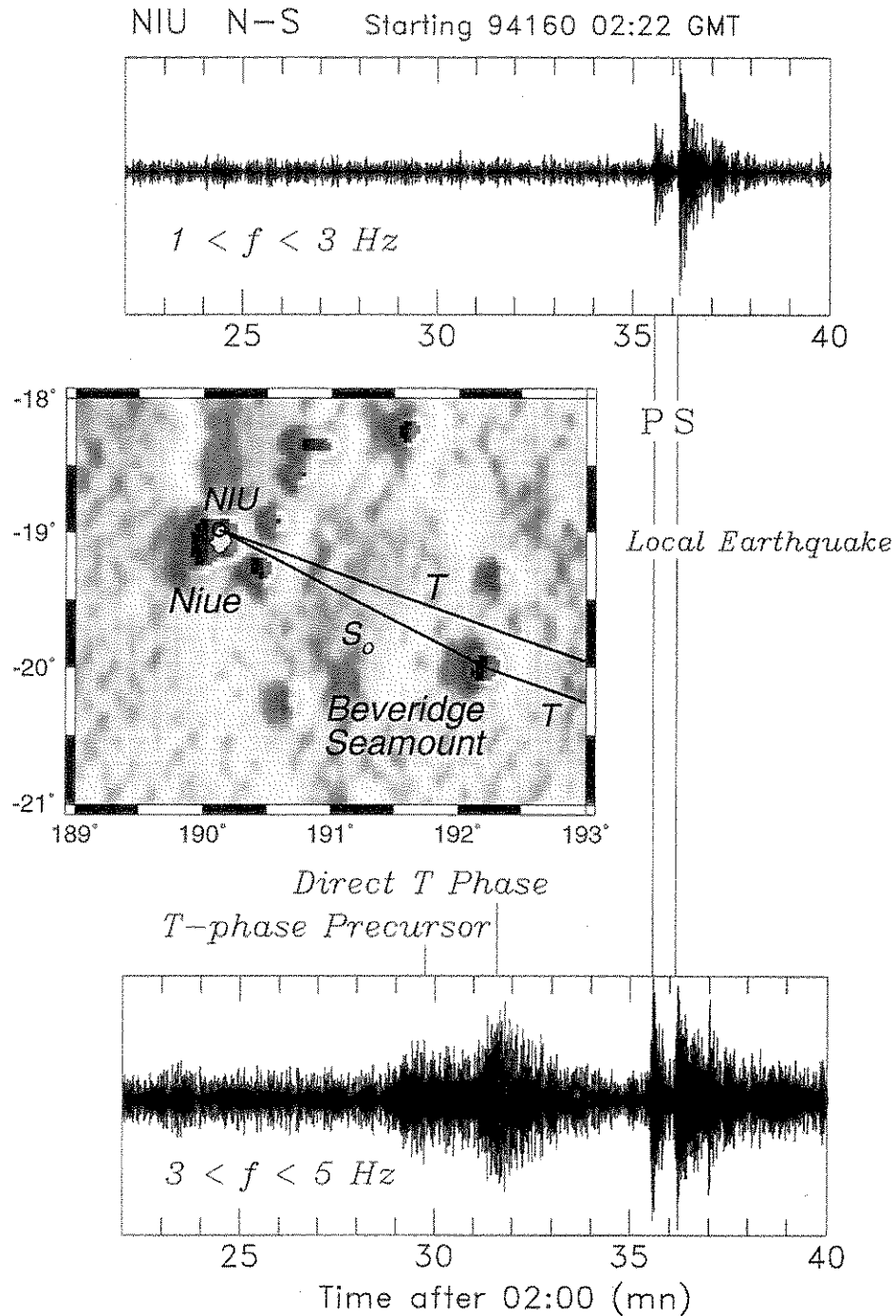


Figure A6b. Same as Figure 2 for Station NAU (Nauru). In this particular figure, the frequency band of the filtered time series is 3–5 Hz.

The timing of this scattered precursor could be compatible with propagation as  $S_0$  between Beveridge and Niue, which could be due to an absence of steep slopes on the scatterer. In this respect, the relative amplitude between the precursor

and the main  $T$  phase would be intermediate between the case of Tetiaroa and Tahiti (Vancouver Island earthquake; small precursor) and Mangaia and Rarotonga (precursor only;  $T$  phase masked), resulting primarily from the relative





**Figure A7.** (top and bottom) Band-pass filtered horizontal (N-S) record at Niue Island. Note that (top) in the 1–3 Hz frequency band, the record is dominated by a local earthquake, whereas (bottom) the  $T$  wave becomes resolvable in a higher-frequency window. (middle) Regional map of free air gravity anomaly in the vicinity of Niue Island [Sandwell and Smith, 1997]. Note that Beveridge Seamount stands out strongly; its maximum signal is  $\sim 1.5 \times 10^{-3} \text{ m/s}^2$ .

sizes of the scattering and receiving edifices. The distance from NIU to the conversion cliff is taken as 10 km, and a correction of 4 s is added to the observed time.

**Acknowledgments.** We thank P. Okubo for access to the HVO data and D. Wiens for providing us with data from his 1994 Tonga-Fiji deployment in advance of general release; S. Tsuboi helped with accessing the POSEIDON data center. Discussions

with R. Russo and S. Beck are also acknowledged. D. James, D. Walker, and C. Kisslinger provided helpful reviews. Several figures were plotted using the GMT software [Wessel and Smith, 1991]. This research is supported by Commissariat à l’Energie Atomique (France). The deployment of the Micronesian stations was supported by the National Science Foundation under Grant EAR-92-18907; their operation was managed by W.P. Richardson, with the local help of L. Skilling (Kosrae) and L. Aingimia (Nauru).

## References

- Beck, S., et al., Across the Andes and along the Altiplano: A passive seismic experiment, *IRIS Newslett.*, XIII (3), 1-3, 1994.
- Cahill, T., and B.L. Isacks, Seismicity and shape of the subducted Nazca plate, *J. Geophys. Res.*, 97, 17503-17529, 1992.
- Engdahl, E.R., R.D. van der Hilst, and J. Berrocal, Imaging of subducted lithosphere beneath South America, *Geophys. Res. Lett.*, 22, 2317-2320, 1995.
- Gilbert, J.F., and A.M. Dziewonski, An application of normal mode theory to the retrieval of structural parameters and source mechanisms from seismic spectra, *Proc. Roy. Soc. London, Ser. A*, 278, 187-269, 1975.
- Helffrich, G.R., S. Stein, and B.J. Wood, Subduction zone thermal structure and mineralogy and their relationship to seismic wave reflections and conversions at the slab-mantle interface, *J. Geophys. Res.*, 94, 753-763, 1989.
- Ihmlé, P.F., and T.H. Jordan, Source time function of the great 1994 Bolivia deep earthquake by waveform and spectral inversions, *Geophys. Res. Lett.*, 22, 2253-2256, 1995.
- Isacks, B.L., and M. Barazangi, High frequency shear waves guided by a continuous lithosphere descending beneath Western South America, *Geophys. J. Roy. astr. Soc.*, 33, 129-139, 1973.
- James, D.E., and J.A. Snoke, Seismic evidence for continuity of the deep slab beneath Central and Eastern Peru, *J. Geophys. Res.*, 95, 4989-5001, 1990.
- Jensen, F.B., W.A. Kuperman, M.B. Porter, and H. Schmidt, *Computational Ocean Acoustics*, 612 pp., Am. Inst. of Phys. Press, New York, 1994.
- Kirby, S.H., E.A. Okal, and E.R. Engdahl: The 09 June 1994 great Bolivian deep earthquake: An exceptional deep earthquake in an extraordinary subduction zone, *Geophys. Res. Lett.*, 22, 2233-2236, 1995.
- Koyanagi, S., K. Aki, N. Biswas, and K. Mayeda, Inferred attenuation from site effect-corrected *T* phases recorded on the Island of Hawaii, *Pure Appl. Geophys.*, 144, 1-17, 1995.
- Linehan, J., S.J., Earthquakes in the West Indian region, *Trans. Amer. Geophys. Un.*, 21, 229-232, 1940.
- Lundgren, P.R., and D. Giardini, The June 9 Bolivia and March 9 Fiji deep earthquakes of 1994: I. Source process, *Geophys. Res. Lett.*, 22, 2241-2244, 1995.
- Mallick, S., and L.N. Frazer,  $P_o/S_o$  synthetics for a variety of oceanic models and their implications for the structure of the oceanic lithosphere, *Geophys. J. Int.*, 100, 235-253, 1990.
- Mammerickx, J., Tectonic framework of the Southcentral Pacific (abstract and map), *Eos, Trans. AGU*, 73, (43), Fall Mtg. Suppl., 586, 1992.
- McLaughlin, *T*-phase observations at San Nicolas Island, California (abstract), *Seismol. Res. Lett.*, 68, 296, 1997 [abstract].
- Piserchia, P.-F., J. Virieux, D. Rodrigues, S. Gaffet, and J. Talandier, A hybrid numerical modeling of *T*-wave propagation: Application the Midplate experiment, *Geophys. J. Int.*, in press, 1997.
- Richardson, W.P., and E.A. Okal, The 1994-1996 Micronesian PASSCAL Experiment: A teleseismic examination of the Ontong-Java Plateau (abstract), *Eos, Trans. AGU*, 77, (22), West. Pac. Mtg. Suppl., W115, 1996.
- Sacks, I.S., Distribution of absorption of shear waves in South America and its tectonic significance, *Yearbook Carnegie Inst. Washington*, 67, 339-344, 1969.
- Sandwell, D.A., and W.H.F. Smith, Marine gravity anomaly from Geosat and ERS-1 satellite altimetry, *J. Geophys. Res.*, 102, 10039-10054, 1997.
- Talandier, J., and M. Bouchon, Propagation of high-frequency  $P_n$  waves at great distances in the Central and South Pacific and its implication for the structure of the lower lithosphere, *J. Geophys. Res.*, 84, 5613-5619, 1979.
- Talandier, J., and G.T. Kuster, Seismicity and submarine volcanic activity in French Polynesia, *J. Geophys. Res.*, 81, 936-948, 1976.
- Talandier, J., and E.A. Okal, Human perception of *T* waves: The June 22, 1977 Tonga earthquake felt on Tahiti, *Bull. Seismol. Soc. Am.*, 69, 1475-1486, 1979.
- Talandier, J., and E.A. Okal, On the mechanism of conversion of seismic waves to and from *T* waves in the vicinity of island shores, *Bull. Seismol. Soc. Am.*, in press, 1997.
- Turner, D.L., and R.D. Jarrard, K-Ar dating of the Cook Austral Islands chain: a test of the hot-spot hypothesis, *J. Volcanol. Geotherm. Res.*, 12, 187-220, 1982.
- Walker, D.A., High-frequency  $P_n$  and  $S_n$  phases recorded in the Western Pacific, *J. Geophys. Res.*, 82, 3350-3360, 1977.
- Walker, D.A., Deep ocean seismology, *Eos, Trans. Amer. Geophys. Un.*, 65, 2-3, 1984.
- Wessel, P., and W.H.F. Smith, Free software helps map and display data, *Eos, Trans. Amer. Un.*, 72, 441, 445-446, 1991.
- Wiens, D.A., P.J. Shore, M. Bevis, K.M. Fischer, K. Draunidalo, G. Prasad, and S.P. Helu, The 1993-1995 Southwest Pacific PASSCAL experiment: deployment and initial results (abstract), *Eos, Trans. AGU*, 75, (16), Spring Mtg. Suppl., 243, 1994.
- Wu, J., T. Wallace, and S. Beck, A very broad band study of the 1994 deep Bolivia earthquake sequence, *Geophys. Res. Lett.*, 22, 2237-2240, 1995.
- Yonekura, N., T. Ishii, Y. Saito, Y. Maeda, Y. Matsushima, E. Matsumoto, and H. Kayanne, Holocene fringing reefs and sea-level change in Mangaia Island, Southern Cook Islands, *Paleogeogr. Paleoclimatol., Paleoecol.*, 68, 177-188, 1988.

E. A. Okal, Department of Geological Sciences, Northwestern University, Evanston, IL 60208. (e-mail: emile@earth.nwu.edu)

J. Talandier, Laboratoire de Détection et Géophysique, Commissariat à l'Énergie Atomique, 91680 Bruyères-le-Châtel, France.

(Received July 2, 1997; revised September 17, 1997; accepted September 23, 1997.)